7698–7710 *Nucleic Acids Research, 2010, Vol. 38, No. 21* *Published online 25 July 2010*
doi:10.1093/nar/gkq635

CPEB2, CPEB3 and CPEB4 are coordinately regulated by miRNAs recognizing conserved binding sites in paralog positions of their 3′-UTRs

Marcos Morgan*, Alessandra Iaconcig and Andrés Fernando Muro*

International Centre for Genetic Engineering and Biotechnology (ICGEB), Padriciano 99, 34149 Trieste, Italy

Received January 26, 2010; Revised and Accepted July 1, 2010

ABSTRACT

The cytoplasmic polyadenylation element binding-protein (CPEB) is an RNA-binding protein that participates in translational control. CPEB2, CPEB3 and CPEB4 are paralog proteins very similar among themselves referred as the CPEB2 subfamily. To gain insight into common mechanisms of regulation of the CPEB2 subfamily transcripts, we looked for putative *cis*-acting elements present in the 3′-UTRs of the three paralogs. We found different families of miRNAs predicted to target all subfamily members. Most predicted target sites for these families are located in paralog positions suggesting that these putative regulatory motifs were already present in the ancestral gene. We validated target sites for miR-92 and miR-26 in the three paralogs using mutagenesis of miRNA-binding sites in reporter constructs combined with over-expression and depletion of miRNAs. Both miR-92 and miR-26 induced a decrease in Luciferase activity associated to a reduction in mRNA levels of the reporter constructs. We also showed that the endogenous miRNAs co-regulate CPEB2, CPEB3 and CPEB4 transcripts, supporting our hypothesis that these genes have a common regulatory mechanism mediated by miRNAs. We also suggest that the ancestral pattern of miRNA-binding motifs was maintained throughout the generation of highly conserved elements in each of the 3′-UTRs.

INTRODUCTION

The 3′-untranslated regions (3′-UTRs) of mRNAs play a central role in the regulation of gene expression in higher eukaryotes. Different *cis*-acting elements within the 3′-UTRs can be recognized by a number of proteic or ribonucleoproteic complexes that can affect the stability, translational activity and/or localization of the mRNAs (1). In vertebrates the cytoplasmic polyadenylation element (CPE) of consensus UUUUUA U is one of the best-characterized sequences within the 3′-UTRs known to participate in the translational activation of mRNAs (2). This element, first studied in *Xenopus laevis* oocyte maturation and later found in other vertebrates including mammals, is recognized by the CPE binding-protein (CPEB). The interaction takes place in the cytoplasm and is responsible for the recruitment of a well-described proteic complex that determines the length of the polyA tail of the mRNAs that have the element [for a review, see (2)]. The length of the PolyA tail correlates with the translational activity of the mRNA (3). In general, translationally dormant mRNAs have short polyA tails while translationally active mRNAs have more elongated ones.

CPEB is the founding member of a family of RNA-binding proteins well conserved in vertebrates. All members of the family contain an N-terminal unstructured region followed by two RNA recognition motifs and a zinc-finger domain towards the carboxy-terminal end of the protein. The protein directly interacts with the CPE through its nucleic-acid-binding domains (4) and interacts with other proteins through the N-terminal regulatory region (2). The other members of the CPEB family in tetrapods, CPEB2, CPEB3 and CPEB4, are very similar at the amino acid sequence of their RNA-binding domains (5) and are referred as the CPEB2 subfamily. Since the three members of the subfamily are present in humans and xenopus the paralogs duplicated before the divergence of the lineages. As CPEB, the CPEB2 subfamily members participate in translational regulation although their recognition elements are different from the CPE (6). All members of the family are abundantly expressed in the brain (5).

*To whom correspondence should be addressed. Tel: +39 040 3757312; Fax: +39 040 226555; Email: muro@icgeb.org
Correspondence may also be addressed to Marcos Morgan. Tel: +39 040 3757312; Fax: +39 040 226555; Email: morgan@icgeb.org

Like the CPEB family members, many different RNA-binding proteins directly interact with mRNAs and regulate their expression. However, mRNA regulation can be also mediated through small RNAs, in particular microRNAs (miRNAs). These small RNAs, 21- to 23-nt long, are present in all higher eukaryotes (7). In animals, they inhibit translation or promote degradation of their target mRNAs by imperfectly binding to their 3′-UTRs (8). Most of the miRNAs specificity in animals is given by nt 2–7, also known as the miRNA seed sequence (9). miRNAs are encoded in the genome and some of them can be grouped in families due to their sequence similarity. Some families, such as the let-7 family, are present in all animals. miRNAs are known to play a central role in a number of key cellular processes such as cellular differentiation (10). Also, dysregulation of the expression of miRNAs has been associated with several pathologies (11). One of the best-studied cases is the over-expression of the miR-17∼92 cluster in certain forms of cancer (12).

Given the high degree of conservation of many abundantly expressed miRNAs different algorithms have been developed to predict target sites in conserved mRNAs (13). The completion during the last decade of several genome-sequencing projects of different phyla made possible to evaluate the conservation throughout evolution of different *cis*-acting elements in regulatory regions. For example, most of the miRNAs prediction programs essentially check the conservation of motifs complementary to seed sequences in ortholog 3′-UTRs. As a result from these studies it has been suggested that many miRNAs can target several hundred messengers. Moreover, most 3′-UTRs have miRNAs target sites (14) underscoring the importance of this regulatory mechanism. In this way, different miRNAs can target the same transcript and, conversely, different mRNAs can be regulated by the same miRNA.

Given the high similarity of the CPEB2 subfamily members, they might have partially overlapping functions. Additionally, as they also have an overlapping expression pattern, they are probably regulated in a similar fashion. For example, all of the subfamily transcripts could be simultaneously bound and regulated by a particular set of miRNAs. To evaluate this hypothesis, we looked for predicted targets for miRNAs present in CPEB2, CPEB3 and CPEB4 mRNAs. Using reporter constructs, we validated binding sites for miR-92 and miR-26 in the three paralogs. Both miRNAs regulate the expression of the reporter constructs by reducing mRNA levels. Depletion of miR-92 alone also induces a modest increase in the levels of the endogenous transcripts. However, depletion of the miRNAs corresponding to the different families that are predicted to co-regulate the transcripts shows a more robust regulation of the endogenous genes. Our results show that these genes have a common regulatory mechanism mediated by miRNAs. We suggest that this mechanism is evolutionary conserved and it was already functional before the generation of highly conserved elements in the 3′-UTRs.

MATERIALS AND METHODS

Bioinformatics

We obtained from the UCSC genome browser web site [http://genome.ucsc.edu/; (15)] the windows depicting the mapping of the last exons of CPEB2, CPEB3 and CPEB4 RefSeq transcripts (16) together with the conservation plots of the genomic regions across different vertebrates. To obtain the frequency of 3′-UTRs with different predicted target sites, we analyzed the Supplementary Data from Lewis *et al.* (17). We considered that a 3′-UTR is targeted when it has at least one conserved sequence complementary to the seed sequence of any miRNA family. To determine the position of the predicted targets in the 3′-UTRs, we followed the TargetScanS rules (17) and mapped each position using multiple alignments of the 3′-UTRs. We did the multiple alignments with the PipMaker program [http://bio.cse.psu.edu/; (18)] under default parameters. In the case of the human CPEB paralogs the final alignment was manually curated due to the low similarity among the sequences.

We downloaded the ESTs mapping to the whole CPEB3 3′-UTR from the UCSC genome browser. We clustered those with sequences finishing within a range of 5 nt from each other. An EST cluster mapping at position ∼2990 from the stop codon was generated around an A-rich sequence encoded in the genome and was excluded from the analysis because it might have been generated by oligo dT miss-priming.

Cell culture

We maintained all cells lines used (K562, CaSKI, GM00637, HACAT, Hep3B, HEK293T, HeLa, SK-N-BE, T98G, MCF-7, U2OS and SA02) at 37°C in an incubator with a humidified atmosphere and a 5.5% concentration of CO_2. We grew the cells in Dulbecco′s Modified Eagle Medium with GlutaMAX, D-Glucose and Pyruvate, supplemented with 10% of fetal calf serum (FCS) and 100 μg/ml of Normicin as an antibiotic/anti-mycotic. We plated regularly passed cells 24 h before transfection. We transfected the cell using Lipofectmine2000 as a transfection reagent following the manufacturers instructions. We transfected the cells when they were 90% confluent. We changed the culture medium to Optimem supplemented with 10% FCS during transfections.

Constructs

To clone the different 3′-UTRs sections, we amplified the regions of interest by PCR from human genomic DNA. We sub-cloned the amplification products inside the pUC vector and examined the presence of undesired mutations by sequencing. We used the following sets of primers: CPEB2 WT dir and rev to amplify CPEB2 WT; CPEB3 WT dir and rev to amplify CPEB3 WT; and CPEB4 WT dir and rev to amplify CPEB4 WT (for the primer's sequences see Supplementary Table S1). To generate the mutated constructs, we amplified these plasmids with mutated primers. Next, we treated the amplifications with DpnI to digest the original wild-type template and we transformed bacteria with the DpnI resistant

mutated plasmids. We then sequenced verified the clones obtained. We used the following primers: CPEB2 Mut92 dir and rev to generate CPEB2 Mut92; CPEB2 Mut26 dir and rev to generate CPEB2 Mut26; CPEB3 Mut92 dir and rev to generate CPEB3 Mut92; and CPEB4 Mut92 dir and rev to generate CPEB4 Mut92 (Supplementary Table S1). We cut the inserts from pUC using XbaI and we cloned the fragments inside the XbaI site of the pGL3-Control vector.

To obtain a vector that over-expresses miR-26a (pSuper-miR-26), we amplified by PCR from human genomic DNA miR-26a precursor using hgDNA miR-26 dir and rev primers. To obtain a vector that over-expresses miR-92a (pSuper-miR-92), we amplified by PCR from human genomic DNA miR-92a precursor using hgDNA miR-92 dir and rev primers. We cloned the amplification products inside a pSuper derived vector linearized with BglII and HindIII.

Luciferase reporter assay

We performed Luciferase reporter assays in 24-well plates. We co-transfected 200 ng of our reporter constructs together with 200 ng of a reporter plasmid encoding for the Renilla Luciferase in order to normalize for the efficiency of transfection. We co-transfected the LNAs at a final concentration of 25 nM (i.e. 12.5 pmol in 500 µl of well volume). LNAs were purchased form Ambion. For co-transfections with miR-26a or miR-92a encoding vectors, we used 100 ng of the reporter vector, 100 ng of the Renilla vector and 200 ng of pSuper-miR-26 or pSuper-miR-92.

We harvested the cells 24 h after transfection by use of the Passive Lysis Buffer from Promega. For the dual Luciferase reporter assay, we used the Luciferase Assay Reagent II and the Stop & Glo Reagent from Promega. We measured luminescence with the 20/20 Luminometer from Turner Biosystems.

RT–qPCR of reporter constructs

We plated SK-N-BE cells in 6-well plates and 24 h later we co-transfected 2.25 µg of the reporter constructs together with 1 µg of the Renilla Luciferase vector. For co-transfections with pSuper-miR-26 or pSuper-miR-92, we transfected 800 ng of the reporter construct, 800 ng of the Renilla vector and 1.6 µg of the corresponding pSuper vector. We harvested the cells 24 h after transfection and extracted total RNA with the TRI reagent solution from Ambion.

In order to eliminate plasmid contamination, we treated 5 µg of total RNA with RNAse free DNAse from Promega. To remove the DNAse after the reaction, we performed an RNA extraction by using the TRI reagent solution from Ambion. We reversed transcribed 800 ng of RNA with the M-MLV reverse transcriptase purchased form Invitrogen.

For the qPCR, we used the following sets of primers: Luc dir and rev to amplify the Luciferase transcript; and Ren dir and rev to amplify the Renilla transcript, at a concentration of 500 nM in a final volume of 20 µl. We used the IQ Custom Syber Green Supermix 2× from BIO-RAD. To perform the reactions, we used a C1000 Thermal Cycler / CFX96 Real time system from Bio-Rad with the following protocol: 30 s at 98°C and 40 cycles of 5 s at 95.0°C and 25 s at 60.0°C. We analyzed the data with the $\Delta\Delta C_t$ method (19) using the Renilla cDNA to normalize for transfection efficiency.

Northern blot analysis for small RNAs

We prepared 13.5% (19:1) acrylamide/bisacrylamide, 5 M Urea, denaturating gels with TBE 1× buffer and loaded 10 µg of total RNA. After the run, we stained the gels with ethidium-bromide and we visualized them with a UV trans-illuminator. We performed semi-dry transfers for 1 h at 2 mA/cm^2 and UV cross-linked the membrane with 1200 µJ. We used LNA oligonucleotides against miR-92a, Let-7a and miR-9 purchased from Ambion and a DNA oligonucleotide against miR-26a of sequence AGCCTATCCTGGATTACTTGAA. To generate the probes, we incubated 2 pmol of the oligonucleotides with 3 pmol of Adenosine 5′-triphosphate [γ-^{32}P] 3000 Ci/mmol in the presence of T4 Kinase for 1 h at 37°C. We performed overnight hybridizations for the LNA and the DNA probes at 60°C and 37°C, respectively, and finally washed the membrane at least three times with SSC 2×, SDS 0.1%.

Northern blot analysis of CPEB3

We prepared total RNA from SK-N-BE cells using the TRI reagent solution from Ambion. We separated 20 µg of RNA in agarose–formaldehyde gels and proceeded as described earlier (20,21). We prepared the probe by PCR amplification from human genomic DNA using the CPEB3-A3dir and CPEB3-A3rev primers. As a marker, we used the 0.5–1 Kb RNA Ladder from Invitrogen.

3′-RACE

We prepared cDNA from 1 µg of total RNA from SK-N-BE cells using Oligo dT as a primer. We performed a first round of PCR amplification of the cDNA with Anchor and CPEB3-5293Dir primers using the following protocol: 3 min at 94°C, followed by 30 cycles of, 30 s at 94°C, 30 s at 56°C and 1 min at 72°C, and a final amplification at 72°C for 10 min. We performed a second PCR repeating the amplification protocol but using the first amplification product as template and CPEB3-5370Dir and Anchor primers. We run the amplification product in an agarose gel, cut the band and sequenced the purified DNA.

RT–qPCR to measure the levels of the endogenous CPEB2, CPEB3 and CPEB4 mRNAs

We amplified cDNA prepared from total RNA of different cell lines using the following primers: GAPDH dir and rev to amplify GAPDH cDNA; CPEB2_1096 dir and CPEB2_1178 rev to amplify CPEB2 cDNA; CPEB3_1575 dir and CPEB3_1690 rev to amplify CPEB3 cDNA; and CPEB4_3127 dir and CPEB4_3261 rev to amplify CPEB4 cDNA. We used GAPDH to normalize the expression levels of CPEB2, CPEB3 and

CPEB4. We used the same amplification conditions as for the reporter constructs.

In order to deplete the endogenous miRNAs, we plated SK-N-BE cells in 12-well plates. We performed a first transfection of 25 nM (i.e. 50 pmol in 2 ml of well volume) of the corresponding LNAs using Lipofectamine2000 24 h after plating the cells and repeated the same transfection 24 h later. Finally, we extracted total RNA after 24 h and synthesized cDNA using random primers. We performed the transfections in duplicates for each treatment.

Statistical analysis

To evaluate the statistical significance between two different treatments, we used the Student's *t*-test.

RESULTS

A novel mRNA isoform of CPEB3 is generated by alternative polyadenylation (APA)

The transcripts of the CPEB2 subfamily members can have 3′-UTRs of more than 3.5 kb [(5); Figure 1A]. Interestingly, an alignment of the human genomic sequences encoding for the CPEB2 subfamily transcripts with the ortholog sequences of other vertebrates showed a high degree of conservation along the entire 3′-UTRs sequences (Figures 1A and 2B) (22). For instance, some regions of the human CPEB2 3′-UTR showed stretches of more than 50 nt perfectly conserved in chicken. Moreover, for CPEB2 and CPEB4 the conservation was completely lost immediately downstream of the genomic region encoding for the cleavage sites (CSs) of the transcripts. However, for CPEB3 we observed a long island of conservation (~950-nt long) located closely downstream of the annotated CS (Figure 1A, empty box). To investigate the transcriptional activity of this region, we looked for the presence of annotated ESTs. We found a number of tags present in this region some of them containing a polyA tail not encoded in the genome and ending ~5520 nt from the stop codon (Supplementary Figure S1A and Table S2). The end of the cluster also matched with the end of the island of conservation (Supplementary Figures S1A and S2B). The other cluster of ESTs that we found along the entire 3′-UTR corresponds to the end of the reference sequence transcript (NM_014912, Supplementary Figure S1A and Table S2).

In order to find cell lines expressing the CPEB2 subfamily members, we performed a screening by using semi-quantitative RT–PCR with specific primers for each gene. All the cell lines tested expressed the three members of the family (Supplementary Figure S3). The expression levels were relatively low but similar among the different subfamily members in each cell line. Since the members of the CPEB2 subfamily have been found in brain (2,5) and the expression levels of the CPEB2 subfamily members in the neuroblastoma SK-N-BE cell line were reasonably high, we selected this cell line to perform all studies shown below (unless otherwise stated). We investigated whether SK-N-BE cells express the newly identified CPEB3 alternative 3′-UTR isoform by Northern blot analysis. Using a probe specific for the new region we detected a band of ~7.8 kb that corresponded to the expected size of CPEB3 mRNA polyadenylated at this novel PAS (Supplementary Figure S1). Additionally, we performed a 3′-RACE experiment followed by sequencing of the PCR product that confirmed the position of the CS found analyzing the ESTs data (Supplementary Figure S2).

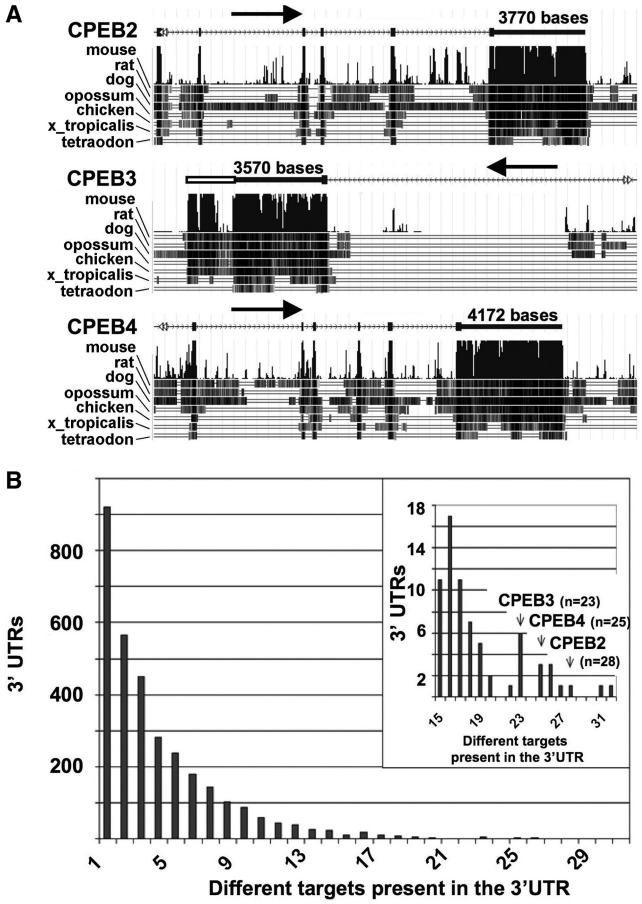

Figure 1. CPEB2 subfamily members have long and conserved 3′-UTRs. (**A**) Mapping of the last exons of human CPEB2, CPEB3 and CPEB4 transcripts to their corresponding genomic sequences visualized with the UCSC genome browser. NCBI Reference Sequences are NM_001177382, NM_014912 and NM_030627 for CPEB2, CPEB3 and CPEB4 transcripts, respectively. Each window spans 20 kb of genomic sequence. The genomic coordinates of the regions shown are chr4:15 053 500–15 073 500, chr10:93 805 000–93 825 000 and chr5:173 370 000–173 390 000 for CPEB2, CPEB3 and CPEB4, respectively. The coordinates correspond to the GRCh37/hg19 assembly of the human genome. On top of each scheme exons are depicted with boxes and introns with thin lines with arrows. The lengths of the longest annotated 3′-UTR variants are indicated above the 3′-UTRs. A conservation plot across different vertebrates is shown for each of the CPEB2 subfamily members. The arrow on top of each scheme indicates the direction of transcription. The empty box downstream of the annotated 3′-UTR of CPEB3 indicates the novel 3′-UTR region. (**B**) Distribution of 3′-UTRs according to the number of different sequences complementary to miRNA seed sequences (conserved in human, mouse, rat, dog and chicken) present in the 3′-UTR as determined by the TargetScanS algorithm (17). An enlargement of the tail of the distribution is shown in the inset. The number of different targets for CPEB2, CPEB3 and CPEB4 is indicated.

CPEB2 subfamily members have an evolutionary conserved pattern of miRNA target sites in their 3′-UTRs

Different groups have developed algorithms to predict binding sites for miRNAs in the 3′-UTRs of different organisms (13). John *et al*. (23) have suggested that CPEB2, CPEB3 and CPEB4 mRNAs are among the transcripts most likely to be targeted by miRNAs in vertebrates. Here, we grouped all human 3′-UTRs according to the number of different miRNA targets predicted by the TargetScanS algorithm (17). The distribution is shown in Figure 1B. Consistently, the analysis of the miRNA targets predicted with this algorithm showed that each of the CPEB2 subfamily members has more than twenty different recognition motifs for miRNAs. As shown in the inset of Figure 1B, CPEB3 is encoded by one of the six transcripts predicted to be bound by 23 different families of miRNAs, CPEB4 transcript is one of the three predicted to be bound by 25 different families of miRNAs and CPEB2 is the only transcript predicted to be bound by 28 different families of miRNAs. Note that each of these families can have one or more binding sites in each 3′-UTR.

Some miRNA families are predicted to have binding sites in more than one member of the CPEB2 subfamily suggesting the existence of a coordinated mechanism of regulation mediated by miRNAs. Indeed, five different families of miRNAs (miR-9, Let-7, miR-26, miR-30 and miR-92) were predicted to bind the three members of the CPEB2 subfamily according to the TargetScanS algorithm (considering miRNA recognition motifs 7- or 8-nt long). This algorithm only considers conservation across orthologs to identify target sites. Thus, the presence of the same target in paralog genes could be explained either by their conservation after the duplication of the paralogs or by convergent evolution. For example, miR-30 predicted binding sites are located in different positions of the 3′-UTRs (Figure 2A) (i.e. close to the stop codon in CPEB2, close to the PolyAdenylation Signal (PAS) in CPEB3 and towards the middle in CPEB4). Therefore, it can be suggested that these sites appeared by convergent evolution. However, for the other four families (miR-9, Let-7, miR-26 and miR-92), we found that they share a common pattern of spatial distribution in the 3′-UTRs of the CPEB2 subfamily (Figure 2A), suggesting that those sites were already present in the ancestral gene. For example, in the three members of the subfamily we identified a putative miR-26/miR-92 doublet target sites close to the PAS. These predicted binding motifs fall in highly conserved regions as shown in Figure 2B for the CPEB2 miR-26/miR-92 doublet. However, when the genomic sequences encoding for the human paralogs were aligned the similarity between the three members was reduced mainly to the sequences that were predicted as putative miRNA recognition motifs (Figure 2C). Importantly, the alignment of the three human paralogs showed a negligible similarity along the entire 3′-UTR sequence (data not shown).

Taken together, these observations suggest that the CPEB2 subfamily members have common predicted miRNA-binding sites located in paralog positions of their 3′-UTRs. Most likely, this pattern was already present in the ancestral gene before gene duplications occurred and it was fixed, in spite of the divergence of the 3′-UTRs observed now among the paralogs. Therefore, the possible order of events regarding the evolution of the 3′-UTRs of the CPEB2 subfamily members is: first, the appearance of miRNA-binding sites in the ancestral CPEB2 gene. Second, the duplication of the paralog genes. Third, the divergence of the paralog sequences without altering the miRNA-binding pattern (Figures 2A and C). Fourth, the radiation of the vertebrates and consequent emergence of ortholog genes. Fifth, the fixation of the whole 3′-UTR sequences in all vertebrates without altering the preexistent miRNA-binding pattern (Figure 2B).

Validation of the distal miR-92 target site in the CPEB2 context

To evaluate the hypothesis of conservation of miRNA target sites after the duplication of the paralogs, we focused our attention on the miR-26/miR-92 doublet, being the targets that most clearly illustrate this possibility. In order to properly dissect the mechanism associated only to this doublet, we studied the last region of the 3′-UTRs (Figures 3A, 4A and 5A and see Supplementary Figure S4 for a summary). In this way, we generated reporter constructs where we cloned the last portion of CPEB2 3′-UTR downstream of the Luciferase gene (CPEB2 WT) (Figure 3A). To evaluate the functionality of the miR-92-binding site of the miR-26/miR-92 doublet, we introduced point mutations to the target motif in the reporter construct (CPEB2 Mut92). We transfected the wild-type and miR-92 mutated constructs into HEK293T and SK-N-BE cells since both cell lines presented high levels of miR-92 (Supplementary Figure S5) and evaluated the activity of both vectors by using the dual Luciferase reporter assay. In both cell lines the activity of the mutated construct was higher than that of the wild-type construct ($P < 0.05$; Figure 3B, left panel). These results are consistent with the role of miRNAs as negative regulators of mRNA expression.

miRNAs are known to reduce the levels of proteins produced by their target transcripts. Although the mechanisms of action are not clearly resolved, in general, miRNAs can control the levels of protein output either by inhibiting translation or by promoting mRNA degradation (8). In order to gain further insight into the mechanism of regulation of CPEB2 3′-UTR, we transfected the wild-type and the miR-92 mutated constructs into SK-N-BE cells and measured the mRNA levels of the reporters by RT–qPCR. The level of Luciferase mRNA was higher for the mutated species ($P < 0.05$; Figure 3B, right panel). These results suggest that miR-92 regulates CPEB2 gene expression by modulating the levels of transcript.

Next, we decided to test the effect of variations in the levels of miRNAs on the activity of our reporter constructs. To this end, we used two complementary approaches. First, we depleted the endogenous miR-92 by transfecting the cells with Locked Nucleic

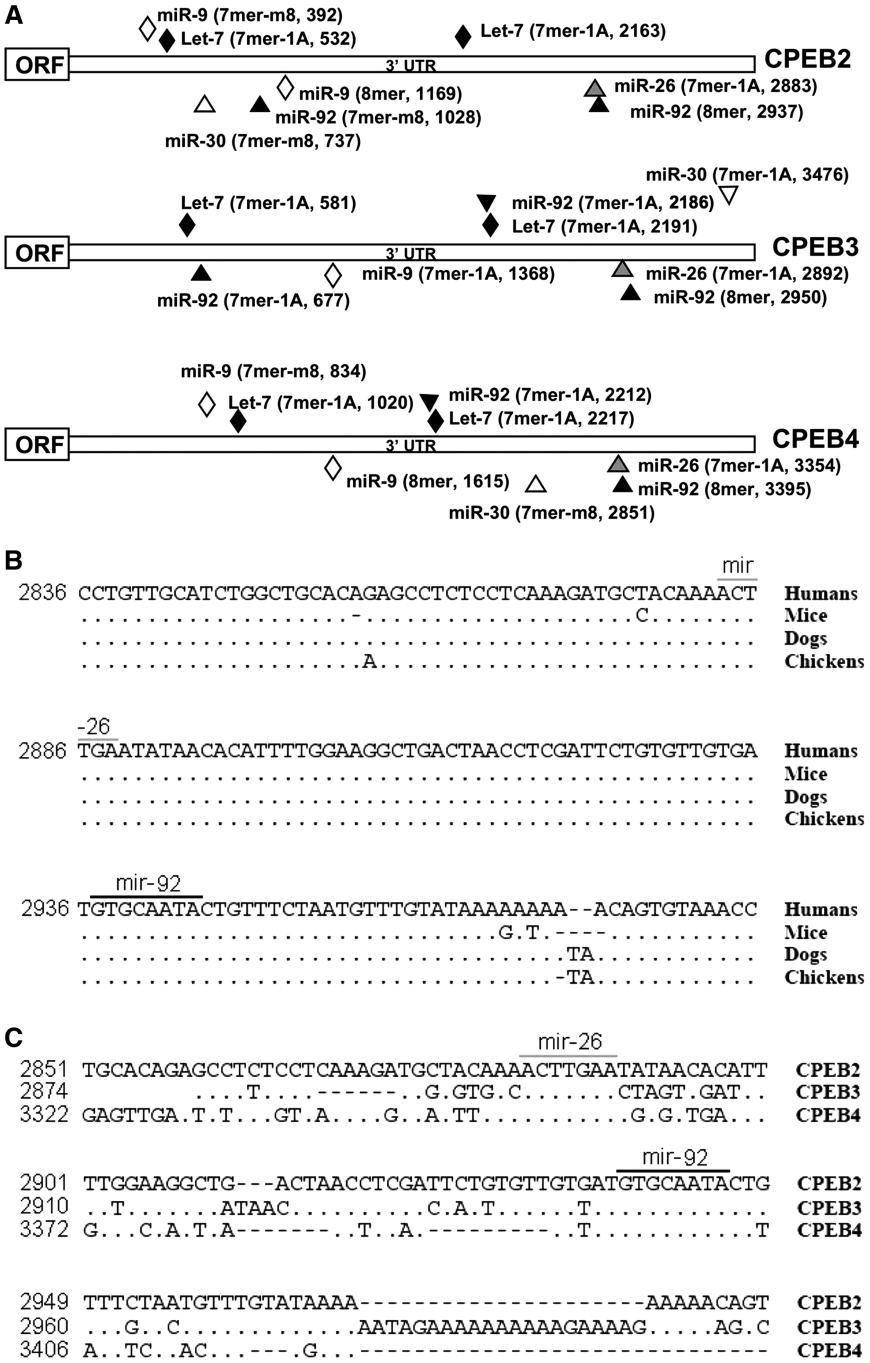

Figure 2. The three members of the CPEB2 subfamily share a similar spatial distribution of common predicted miRNA targets. (**A**) The distribution of binding sites corresponding to the five miRNA families that are predicted to have at least one binding site in each of the CPEB2 subfamily transcripts is shown. Between brackets the type of predicted target and the position in the 3′-UTR is shown. (7mer-1A, target complementary to a miRNA seed sequences flanked by a conserved A immediately downstream; 7mer-m8, target complementary to an extended seed sequence; 8mer, target complementary to an extended seed sequence flanked by a conserved A immediately downstream). (**B**) Multiple alignment of part of human, mouse, dog and chicken CPEB2 3′-UTRs obtained by using the PipMaker program (18). The nucleotide position with respect to the stop codon is shown for humans. Conserved bases are represented with dots and indels with horizontal bars. miR-26 and miR-92 predicted targets are indicated. (**C**) Alignment of the same region of the human CPEB2 3′-UTR with human CPEB3 and CPEB4 3′-UTRs. The nucleotide position with respect to the stop codon is shown on the left. The predicted target motifs for miR-92 and miR-26 are shown.

Acids (LNAs) complementary to the mature miRNA sequence and, second, we over-expressed miR-92 by transfecting the cells with a pSuper derived vector containing the genomic region encoding miR-92 precursor under the control of the H1 promoter (pSuper-miR-92). We first verified by Northern blot analysis the levels of miR-92 in the cells after the treatments (Figure 3C). Transfection of SK-N-BE cells with the miR-92 specific LNA

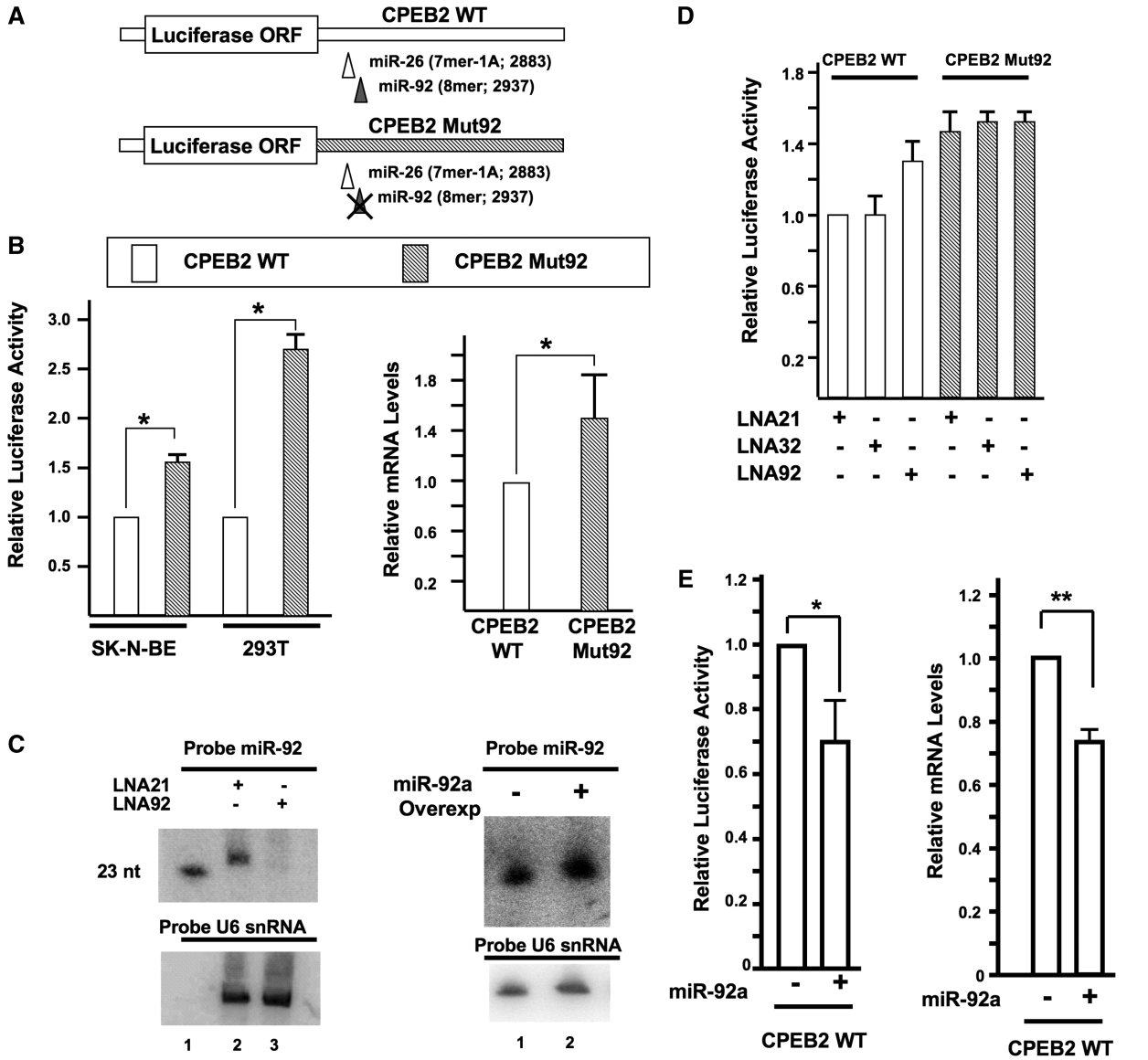

Figure 3. Validation of the distal miR-92-binding site of CPEB2 3′-UTR using reporter constructs. (**A**) Scheme of the reporter constructs used. The last portion of CPEB2 3′-UTR, from base 2497 onwards (with respect to the stop codon), was cloned downstream of the Luciferase gene (CPEB2 WT). Point mutations were introduced to the miR-92 target site (CPEB2 Mut92) in an analogous construct. The type and the position of the target in the wild-type 3′-UTR are indicated between brackets. (**B**) Left panel; relative Luciferase activity of the reporter constructs transfected into SK-N-BE and HEK293T cells. The mean of three independent transfections is shown. Right panel; quantification of Luciferase mRNA levels by RT–qPCR from SK-N-BE cells transfected with the reporter constructs. CPEB2 Mut92 mRNA levels are normalized to those of CPEB2 WT. The mean of five independent transfections is shown. (**C**) Left panels: Northern blot analysis for small RNAs of total RNA from SK-N-BE cells transfected with LNAs complementary to miR-92 or miR-21. The membrane hybridized with a probe complementary to miR-92 is shown in the upper panel. A DNA oligonucleotide with miR-92 sequence was run in parallel as a molecular weight marker (Lane 1). The same membrane, after stripping and hybridization with a specific probe against U6, is shown in the lower panel. Right panels: Northern blot analysis for small RNAs of total RNA from SK-N-BE cells transfected with pSuper-miR-92 or the empty vector. (**D**) Luciferase activity of the constructs co-transfected with LNAs against miR-21, miR-32 or miR-92 in SK-N-BE cells. The mean of three independent transfections is shown. Values shown are relative to CPEB2 WT activity co-transfected with the LNA against miR-21. (**E**) Left panel; Luciferase activity of CPEB2 WT construct co-transfected with pSuper-miR-92. Right panel; mRNA levels of CPEB2 WT construct co-transfected with pSuper-miR-92. The mean of four independent transfections is shown. In all cases a Renilla Luciferase expressing vector was used to normalize for the efficiency of transfection. The statistical significance was tested by using the Student's *t*-test ($*P < 0.05$, $**P < 0.01$). Error bars indicate 1 SD.

resulted in an efficient depletion of the endogenous miRNA while a control LNA against miR-21 did not affect the endogenous miR-92 levels (Figure 3C, left panel). Transfection of the cells with pSuper-miR-92 resulted in an increase of miR-92 levels (Figure 3C, right panel).

When we co-transfected the wild-type and mutated CPEB2 reporter vectors together with the unspecific LNA21, the activity of the CPEB2 Mut92 vector was higher (Figure 3D, compare the first and fourth bars). However, when we co-transfected miR-92 specific LNA with the reporter constructs, the Luciferase activity

of the wild-type reporter construct increased to levels similar to those of the mutated one (Figure 3E, compare the third and sixth bars). Thus, depleting the cells of the specific miRNA or mutating its putative binding site had similar effects on the 3′-UTR-mediated regulation of CPEB2 reporter constructs. Additionally, we used an LNA against miR-32 that can also recognize the same seed motif as miR-92 although their sequences are significantly different. In this case, we observed no effect of the LNA on the Luciferase activity of the wild-type reporter construct. These results were confirmed by the over-expression of miR-92 that resulted in a 30% decrease of both Luciferase activity and mRNA levels (Figure 3E). Taken together, these findings indicate that miR-92 binds to its predicted recognition motif in the 3′-UTR of CPEB2 and the observed down regulation in protein synthesis of the CPEB2 WT reporter construct can be attributed, at least in part, to a decrease in the levels of transcript.

Validation of the distal miR-92 target sites in CPEB3 and CPEB4 3′-UTRs

The validation of the distal miR-92 target site in the CPEB2 context prompted us to study its functionality in the other paralog genes of the subfamily. To this end, we cloned the last region of CPEB3 and CPEB4 RefSeq 3′-UTRs in a reporter vector downstream of the Luciferase gene (CPEB3 WT and CPEB4 WT respectively). We also generated analogous constructs introducing point mutations into the predicted recognition sequences for miR-92 (CPEB3 Mut92 and CPEB4 Mut92) (Figure 4A). Then, we transfected HEK293T and SK-N-BE cells with the reporter vectors. In each case, the Luciferase activity was higher for the mutated reporter constructs (Figure 4B).

Depletion of the endogenous miR-92 with a specific LNA produced an increase in the Luciferase activity of the wt constructs, while no variations were observed for the miR-92 mutant constructs (Figure 4C and E). Supporting the previous results, over-expression of miR-92 resulted in a decrease of Luciferase activity for the wild-type CPEB3 and CPEB4 constructs but not for the mutant ones (Figure 4D and F). Together, these results suggest that the most distal miR-92 site is functional in all of the CPEB2 subfamily members.

Validation of miR-26 target sites in the different paralogs

Next, we wanted to investigate the functionality of the miR-26 predicted target site located in close proximity to the distal miR-92 motif in the CPEB2 context. In order to increase the levels of miR-26 in neuroblastoma cells, we adopted the same strategy used for miR-92. We cloned the genomic region encoding miR-26 precursor in the pSuper derived vector described above (pSuper-miR-26). When we transfected pSuper-miR-26 into SK-N-BE cells the levels of miR-26 increased considerably (Figure 5B). To evaluate the effects of miR-26 over-expression, we co-transfected pSuper-miR-26 together with CPEB2 WT. The Luciferase activity decreased when the miRNA was over-expressed (Figure 5C, compare the first two bars). To validate the specificity of the interaction, we introduced point mutations into the reporter construct at the level of the miR-26 predicted target site (CPEB2 Mut26, Figure 5A). In this case, we observed that the Luciferase activity of the mutant construct did not change when the miRNA was over-expressed (Figure 5C, compare the last two bars). These results indicate that miR-26 binds to CPEB2 3′-UTR at the level of the predicted target reducing CPEB2 protein levels.

In order to gain further insight into the mechanisms of regulation mediated by miR-26, we measured by RT–qPCR the mRNA levels of CPEB2 WT when miR-26 was over-expressed. We observed a decrease in the amount of the reporter messenger when the miRNA levels increased (Figure 5D). Thus, as with miR-92, miR-26 mediated reduction in protein output is, at least partially, due to a decrease in the levels of Luciferase mRNA. In summary, the results obtained using the Luciferase reporter constructs suggest that both miR-26 and miR-92 predicted target sites analyzed are functional and regulate CPEB2 gene expression.

To validate the predicted miR-26-binding sites in CPEB3 and CPEB4, we co-transfected into SK-N-BE cells the wild-type reporter constructs together with pSuper-miR-26. We observed a decrease in Luciferase activity associated to the increase in miR-26 levels in both cases (Figure 5E), as we previously observed for the CPEB2 reporter. Thus, these results are in agreement with the existence of functional miR-26-binding sites in the last region of CPEB3 and CPEB4 3′-UTRs. Taken together, these observations favor a model in which the three members of the CPEB2 subfamily; CPEB2, CPEB3 and CPEB4, are regulated by miR-26 and miR-92. These miRNAs bind to paralog positions of the transcripts and down-regulate their expression.

Coordinated regulation of the endogenous CPEB2, CPEB3 and CPEB4 mRNAs by miRNAs

We have shown above that miR-92 and miR-26 are able to regulate the expression levels of reporter genes containing the 3′-terminal portion of CPEB2, CPEB3 and CPEB4 3′-UTRs. To have a deeper insight into the miRNA-mediated regulation of the CPEB2 subfamily of mRNAs and extend the results obtained so far to the other families of miRNAs presumably targeting the three paralogs, we measured the levels of the endogenous transcripts after depleting the cells of their endogenously expressed miRNAs. To this end, we used specific LNAs directed against miR-92, or a mix of LNAs directed against the four miRNA families which have predicted binding sites in paralog positions of all three members of the CPEB2 subfamily (Figure 2): miR-26, Let-7, miR-9 and miR-92.

Depletion of miR-92 showed a modest (15–20%) but significant increase in the endogenous mRNA levels of all three subfamily members measured by RT–qPCR (Figure 6B) in agreement with the evolutionary analysis and the results obtained with the reporter constructs. Transfection of SK-N-BE cells with the LNAs mix

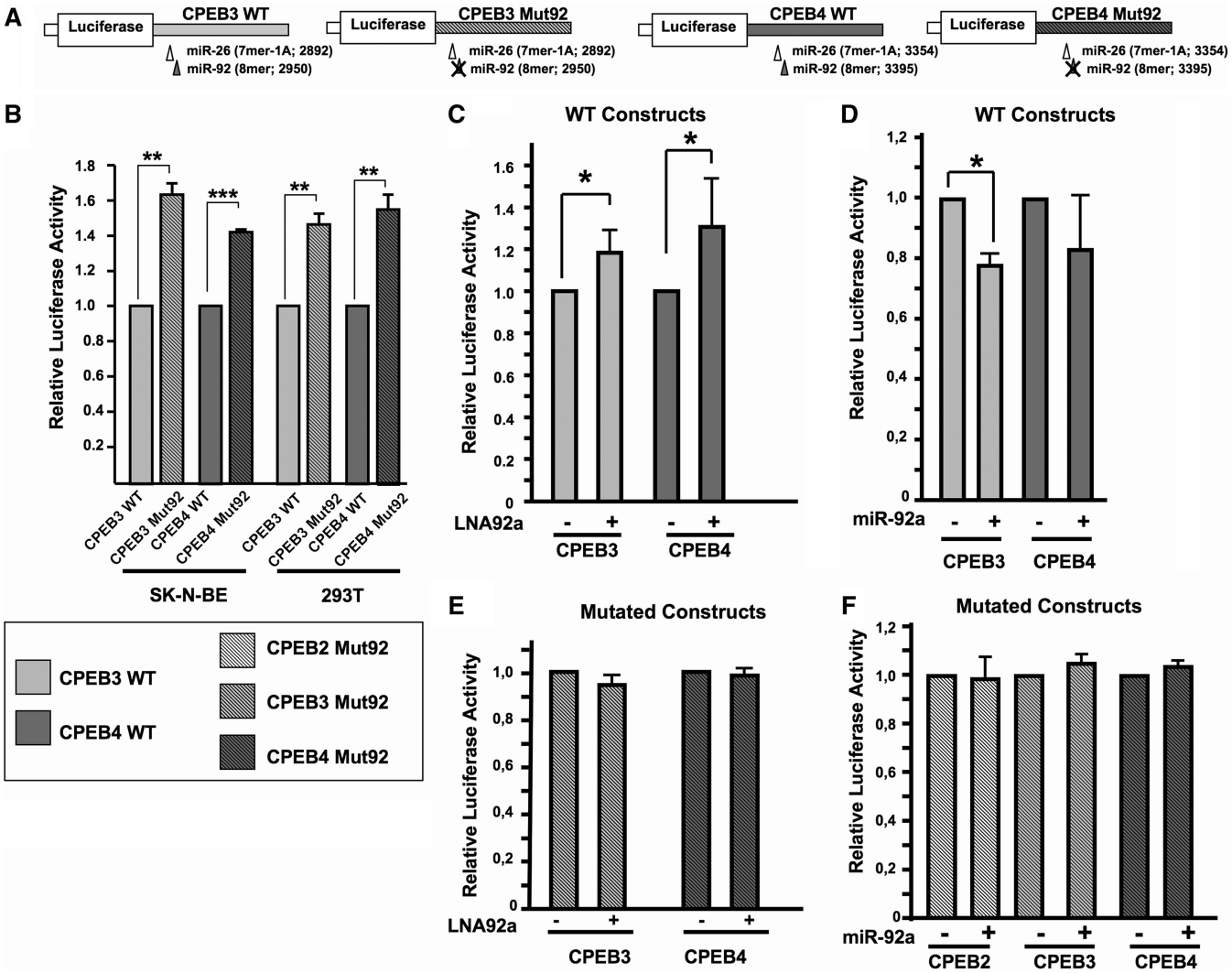

Figure 4. Validation of the distal miR-92 predicted targets in paralog positions of CPEB3 and CPEB4 3′-UTRs. (**A**) Scheme of the reporter constructs used. The last segments of CPEB3 and CPEB4 3′-UTRs, from bases 2779 and 3177 onwards, respectively (with respect to the stop codon), were cloned downstream of the Luciferase gene (CPEB3 WT and CPEB4 WT respectively). Analogous constructs with point mutations in the miR-92 target sequence were also generated (CPEB3 Mut92 and CPEB4 Mut92). The type and the position of the target in the wild-type 3′-UTRs are indicated between brackets. (**B**) Relative Luciferase activity of the reporter constructs transfected into SK-N-BE and HEK293T cells. The mean of three independent transfections is shown. (**C**) and (**E**) Luciferase activity of CPEB3 WT and CPEB4 WT (C) or CPEB3 Mut92 and CPEB4 Mut92 reporter constructs (E) co-transfected with an LNA against miR-92a or a control LNA against miR-21. The mean of four independent experiments is shown. (**D**) and (**F**) Luciferase activity of CPEB3 WT and CPEB4 WT (D) or CPEB2 Mut92, CPEB3 Mut92 and CPEB4 Mut92 constructs (F) co-transfected with pSuper-miR-92 or the empty vector. The mean of four independent experiments is shown. Reporter constructs were always co-transfected with a vector encoding the Renilla Luciferase to normalize for the efficiency of transfection. The statistical significance was evaluated using the *t*-test (*$P < 0.05$; **$P < 0.01$; ***$P < 0.001$). Error bars indicate 1 SD.

resulted in the almost complete depletion of miR-26a, Let-7a, miR-9 and miR-92a (Figure 6A). The simultaneous depletion of miRNAs produced a more robust increase in the levels of the transcripts ranging from 30% for CPEB3 to 45% for CPEB4, with CPEB2 showing an intermediate increase of 40% (Figure 6C). In this way, by depleting the endogenously expressed miRNA and measuring the levels of the endogenous transcripts we provided further evidence that the CPEB2 subfamily members can be coordinately regulated by a common subset of miRNAs that simultaneously recognize miRNA-binding sites located in paralog positions of their 3′-UTRs

DISCUSSION

In this work, we have provided evidence that gene expression of the CPEB2 subfamily is coordinately regulated by a group of miRNAs. CPEB2, CPEB3 and CPEB4 are paralog genes each one having a very high number of predicted miRNA-binding sites in its 3′-UTR according to the TargetScanS algorithm (17). These sites are predicted on the basis of their conservation across ortholog genes. Therefore, target prediction is independent between paralogs for this algorithm. In this way, considering only those targets present in all three members of the CPEB2 subfamily, we added another step of stringency to our analysis. Interestingly, four out of five

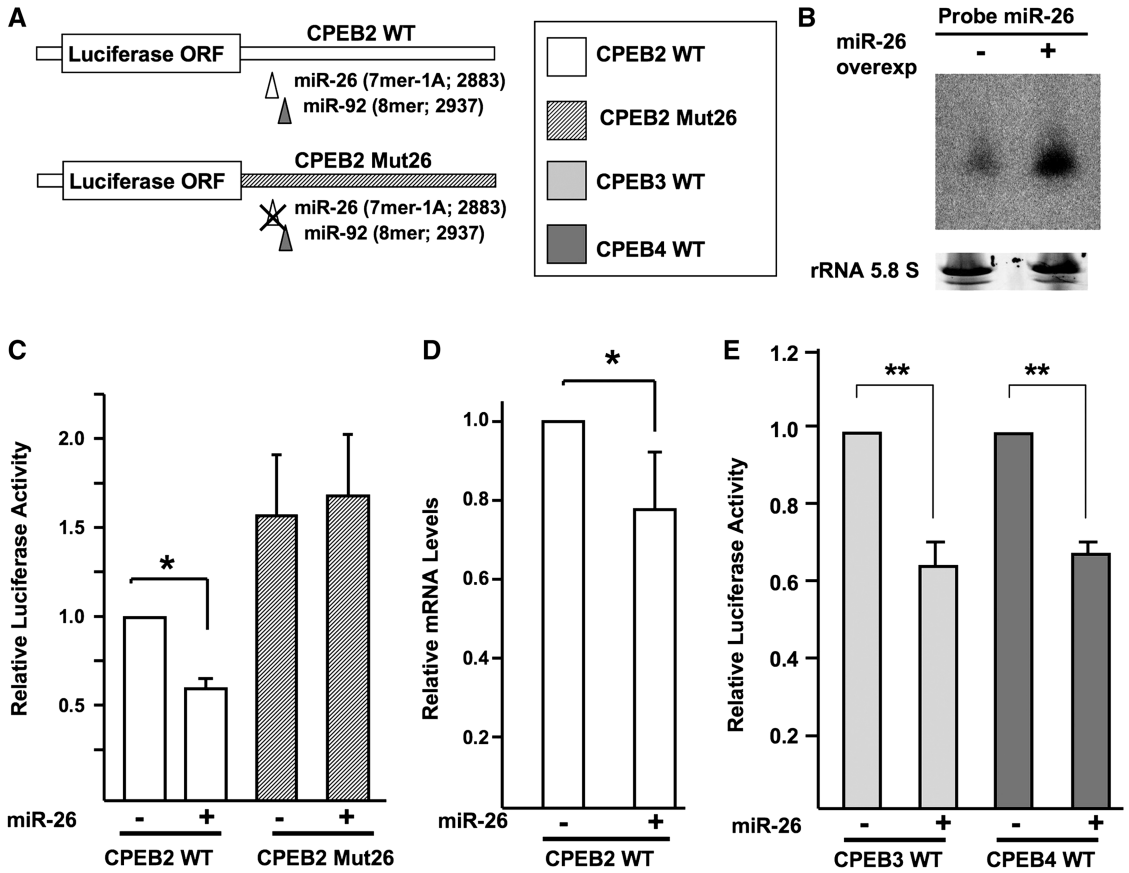

Figure 5. Validation of miR-26-binding sites using reporter constructs. (**A**) Scheme of the reporter constructs used. The predicted miR-26 target site in CPEB2 was mutated by site-directed mutagenesis (CPEB2 Mut26). The type and position of the target in the WT 3′-UTR are indicated between brackets. (**B**) Northern blot analysis for small RNAs of SK-N-BE cells transfected with pSuper-miR-26 or the empty vector. The membrane was hybridized with a probe specific for miR-26a (upper panel). The lower panel shows the 5.8S rRNA band in the gel used as a loading control. (**C**) Relative Luciferase activity of the reporter constructs co-transfected with pSuper-miR-26. The mean of three independent transfections is shown. (**D**) Quantification of Luciferase mRNA levels by RT–qPCR from SK-N-BE cells co-transfected with CPEB2 WT reporter construct and pSuper-miR-26 or the empty vector. The mean of five independent transfections is shown. Values are normalized to CPEB2 WT transcripts transfected with the empty vector. (**E**) Relative Luciferase activity of CPEB3 WT and CPEB4 WT reporter constructs co-transfected with pSuper-miR-26 or the empty vector into SK-N-BE cells. The mean of three independent transfections is shown. Reporter constructs were always co-transfected with a vector encoding the Renilla Luciferase to normalize the efficiency of transfection. The statistical significance was evaluated using the *t*-test (*$P < 0.05$; **$P < 0.01$). The error bars indicate 1 SD.

miRNA families with target sites in all members of the subfamily showed a similar positional distribution of their binding sites (miR-9, Let-7, miR-26 and miR-92, Figure 2A). This observation strongly suggests that these regulatory motifs were already functional in the ancestral gene and were maintained after gene duplications in all tetrapods. The conservation of these motifs in the three members of the subfamily and in different species suggests that there is a strong selective pressure on these regions. Indeed, when the genomic sequences encoding for the 3′-UTR of different orthologs were aligned the conservation was extremely high and extended to the sequences flanking the individual miRNA target sites. However, the divergence at the sequence level of the different paralogs suggests that the target sites were already present before the generation of highly conserved elements in the 3′-UTRs. Interestingly, this high conservation is lost downstream of the CS in all the CPEB2 subfamily members. This suggests that the regulatory elements under strong evolutionary selection are part of the mRNA itself and not of the genomic region. This seems to be true for most conserved elements in genomic sequences encoding for 3′-UTRs (24). CPEB 3′-UTR is also conserved all throughout its sequence. However, while the 3′-UTRs of the CPEB2 subfamily members are more than 3.5-kb long, CPEB 3′-UTR is only 1390-nt long. The CPEB transcript is also a predicted target of miR-92, miR-9 and Let-7 suggesting a simultaneous regulation of all the members of the family. However, the distribution of the putative miRNA-binding sites is different to the one observed for CPEB2, CPEB3 and CPEB4 (data not shown).

The widespread presence of miRNAs in higher eukaryotes suggests that they play an important role in the regulation of gene expression. While in plants endogenous small RNAs can perfectly bind and induce the cleavage of their targets, the situation in animals is different (7). In the latter case, the binding of the miRNA is imperfect and changes in the target translational activity are not always drastic. In animals, miRNAs can regulate the

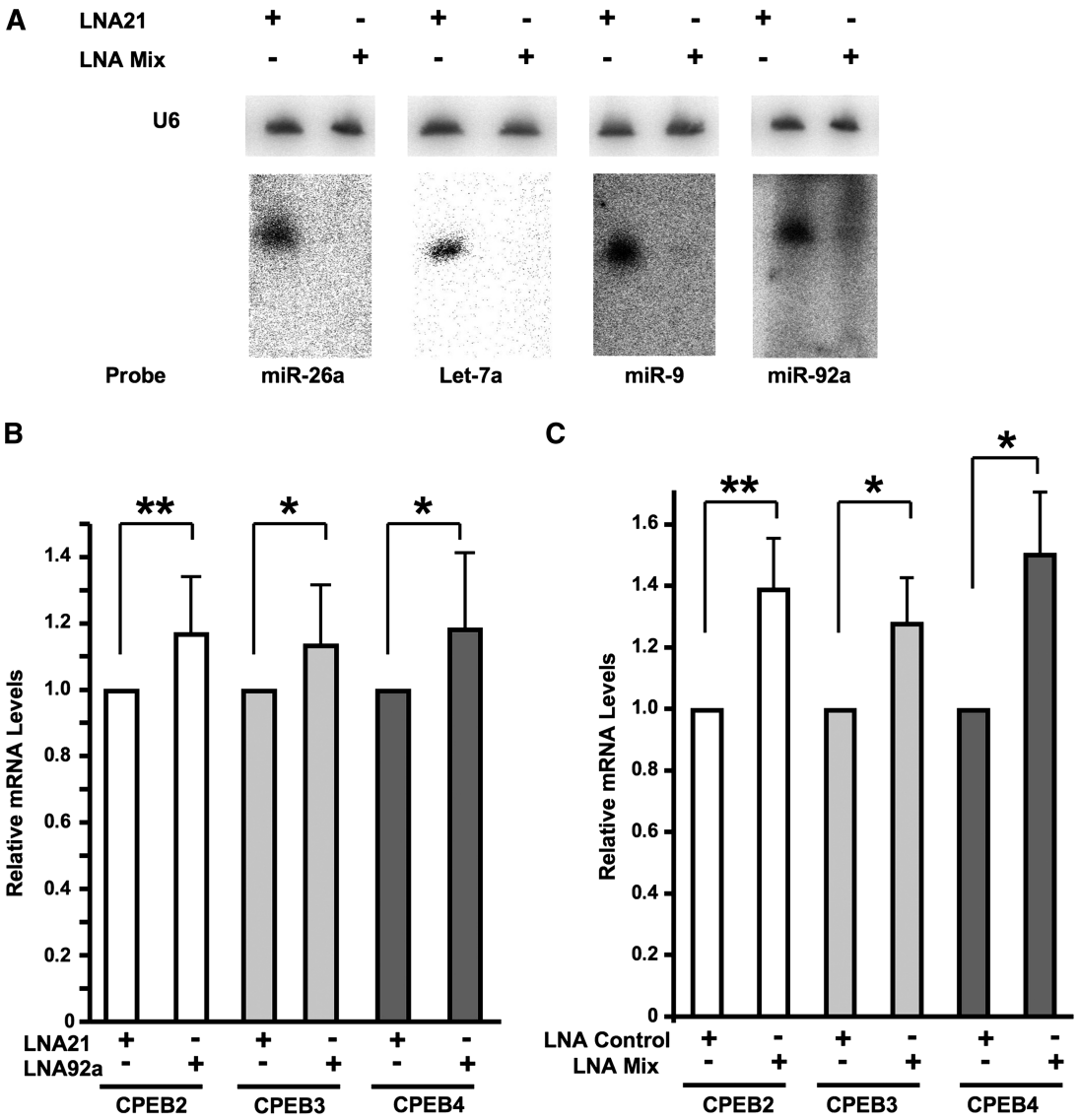

Figure 6. Co-regulation of the endogenous CPEB2, CPEB3 and CPEB4 transcripts by endogenously expressed miRNAs. (**A**) Total RNA samples extracted from SK-N-BE cells transfected with a mix of LNAs against miR-92a, miR-26a, Let-7a and miR-9 (LNA Mix) or an LNA against miR-21 were run in parallel, except for the one used to detect miR-92a that corresponds to the stripped membrane used for miR-26a. The membranes were hybridized with specific probes for the indicated miRNAs. U6 RNA was used as a loading control. (**B**) RT–qPCR of RNA obtained from SK-N-BE cells transfected with an LNA against miR-92 or miR-21. The values are the average of eight or more independent experiments performed in duplicates. (**C**) RT–qPCR of RNA prepared from SK-N-BE cells transfected with an LNA against miR-21 (LNA Control) or a mix of LNAs against miR-92a, Let-7a, miR-26a or miR-9 (LNA Mix). The values are the average of four independent experiments performed in duplicates. GAPDH was used to normalize the levels of the endogenous CPEB2, CPEB3 and CPEB4 transcripts. The statistical significance was evaluated using the *t*-test (*$P < 0.05$; **$P < 0.01$). The error bars represent 1 SD.

activity of their target transcripts through different mechanisms such as translational repression and mRNA degradation (8). More recently, miRNAs were also shown to induce deadenylation of their targets (25–27). Given the high number of predicted targets for each miRNA it is not yet clear whether they act by affecting the translational activity of many transcripts, or by affecting a few key targets, or something in between. Transcripts encoding for nucleic-acid-binding proteins tend to be enriched in predicted targets (9). In this sense, it is interesting to notice that the CPEB2 subfamily members, that are suggested to be involved in translational regulation, appeared to be particularly regulated by miRNAs.

RNA-binding proteins are the other key players in 3′-UTR regulation. Their binding motifs are in some cases more relaxed than those of miRNAs rendering more difficult to predict their *cis*-acting elements from the 3′-UTR primary sequence. Many regulatory proteins interact with sequences with high A/U content usually referred as AU rich elements (28). Some studies have shown that there can be a coordinated regulation by miRNAs and RNA-binding proteins. For example, Bhattacharyya *et al.* (29) have shown that CAT-1 gene

expression is regulated by the coordinated action of miR-122 and HuR. Other study has proposed that in the germ line Dnd1 can directly interfere with miRNA mediated regulation by competing for their binding sites in 3′-UTRs (30). In this way, particular targets can escape inhibition mediated by co-expressed miRNAs. In both cases, HuR and Dnd1 bind to regions of high A/U content. The CPEB2 subfamily transcripts have conserved A/U enriched sequences. In particular, their 3′-UTRs have conserved CPEs, as shown in Supplementary Figure 4. Recently it has been shown that the *Xenopus laevis* CPEB4 transcript is regulated by CPEs present in its 3′-UTR (31). Therefore, these mRNAs might be bound and regulated by different proteins such as the CPEB2 subfamily members themselves. Thus, the steady state levels of the transcripts might not only be determined by miRNAs but also by co-expressed RNA-binding proteins. This could in part explain why not always an inverse correlation between the levels of the CPEB2 subfamily transcripts and their regulatory miRNAs is observed across different cell lines (Supplementary Figures S3 and S5).

MiR-26 and miR-92 families have several members and are well conserved in vertebrates. As the Let-7 family, the miR-92 family is also present in invertebrates. Moreover, the octamer motif complementary to miR-92 seed sequence has an extremely high rate of conservation in vertebrates (24). Some of the miR-92 members are encoded in three paralog clusters in the mammalian genomes (32). Knockout mice of the three clusters show premature mortality underscoring the importance of these miRNAs in developmental control (33). Additionally, over-expression of the cluster can lead to cancer development (12). MiR-26 has also been involved in cancer development by targeting genes such as PTEN and EZH2 (34,35).

The prediction of miRNA targets is still under development and different approaches, including conservation analysis, structural studies, and functional assays are being used and combined (36). In this study, we showed that the conservation of predicted targets, not only in ortholog genes, but also in paralogs could be used as an additional tool to identify real targets. In the case of the CPEB2 subfamily, a number of sites seem to be common to two or three of the members. However, this might be an exception due to the relatively long and conserved 3′-UTRs of each of the CPEB2 subfamily paralogs. Nevertheless, it could be possible that other transcripts encoding for a group of paralog proteins, with presumably overlapping functions, are also coordinately regulated by one or more miRNAs.

APA can generate transcripts of different lengths where the shorter isoforms may lack regulatory elements present in the longer ones. In our laboratory, we have previously shown that the β-adducin pre-mRNA can undergo APA (37). In this gene, the usage of a proximal PAS in erythroid tissues generates transcripts of approximately 3- to 4-kb long. Instead, the utilization in brain of a more distal PAS gives rise to an unusually long mRNA of 8-kb with a 3′-UTR of more than 6-kb (37). The short β−adducin transcript isoform showed a relief in gene expression due to the loss of regulatory elements (A.F.M., unpublished results). Recent papers provided evidence that this is a general phenomenon associated to proliferation and is necessary to escape the tight regulation mediated by long 3′-UTRs. It was shown that actively dividing cells tend to have shorter 3′-UTRs compared to differentiated cells (38,39). Additionally, 3′-UTRs shortening has been implicated in cancer progression underscoring the importance of APA from a clinical point of view (40).

However, as we showed before for β-adducin and in this work for CPEB3, PAS are not exhaustively annotated. Wide genome analyses of polyA sites and alternative 3′-UTR isoforms strongly rely on transcriptional data [e.g. (41,42)]. In the case of CPEB3 the striking conservation of the genomic sequence was a good enough indicator of the existence of a novel alternative 3′-UTR isoform that was further confirmed by bioinformatics and biochemical analyses (Supplementary Figures S1 and S2). The alternative PAS is downstream of the identified miRNA targets that co-regulate the different subfamily members. Therefore, independently of which of these PASs is used, the CPEB3 mRNA can be always co-regulated together with CPEB2 and CPEB4.

SUPPLEMENTARY DATA

Supplementary Data are available at NAR Online.

ACKNOWLEDGEMENTS

The authors thank all members of their and Prof. F. Baralle′s groups for their help throughout the work. The authors thank Dr Alessandro Carrer for his valuable help with the RT–qPCR experiments, Dr Emanuele Buratti for critical reading of the manuscript and Dr Klaus Förstemann for the small RNAs Northern blot analysis protocol.

FUNDING

Funding for open access charge: International Centre for Genetic Engineering and Biotechnology intramural funding.

REFERENCES

1. Mignone,F., Gissi,C., Liuni,S. and Pesole,G. (2002) Untranslated regions of mRNAs. *Genome Biol.*, **3**, reviews0004.0001–reviews0004.0010.
2. Richter,J.D. (2007) CPEB: a life in translation. *Trends Biochem. Sci.*, **32**, 279–285.
3. Sachs,A.B., Sarnow,P. and Hentze,M.W. (1997) Starting at the beginning, middle, and end: translation initiation in eukaryotes. *Cell*, **89**, 831–838.
4. Hake,L.E., Mendez,R. and Richter,J.D. (1998) Specificity of RNA binding by CPEB: requirement for RNA recognition motifs and a novel zinc finger. *Mol. Cell Biol.*, **18**, 685–693.
5. Theis,M., Si,K. and Kandel,E.R. (2003) Two previously undescribed members of the mouse CPEB family of genes and their inducible expression in the principal cell layers of the hippocampus. *Proc. Natl Acad. Sci. USA*, **100**, 9602–9607.
6. Huang,Y.S., Kan,M.C., Lin,C.L. and Richter,J.D. (2006) CPEB3 and CPEB4 in neurons: analysis of RNA-binding specificity and

translational control of AMPA receptor GluR2 mRNA. *EMBO J.*, **25**, 4865–4876.
7. Bartel,D.P. (2004) MicroRNAs: genomics, biogenesis, mechanism, and function. *Cell*, **116**, 281–297.
8. Pillai,R.S., Bhattacharyya,S.N. and Filipowicz,W. (2007) Repression of protein synthesis by miRNAs: how many mechanisms? *Trends Cell. Biol.*, **17**, 118–126.
9. Lewis,B.P., Shih,I.H., Jones-Rhoades,M.W., Bartel,D.P. and Burge,C.B. (2003) Prediction of mammalian microRNA targets. *Cell*, **115**, 787–798.
10. Schickel,R., Boyerinas,B., Park,S.M. and Peter,M.E. (2008) MicroRNAs: key players in the immune system, differentiation, tumorigenesis and cell death. *Oncogene*, **27**, 5959–5974.
11. Jiang,Q., Wang,Y., Hao,Y., Juan,L., Teng,M., Zhang,X., Li,M., Wang,G. and Liu,Y. (2009) miR2Disease: a manually curated database for microRNA deregulation in human disease. *Nucleic Acids Res.*, **37**, D98–D104.
12. Mendell,J.T. (2008) miRiad roles for the miR-17-92 cluster in development and disease. *Cell*, **133**, 217–222.
13. Rajewsky,N. (2006) microRNA target predictions in animals. *Nat. Genet.*, **38(Suppl.)**, S8–S13.
14. Friedman,R.C., Farh,K.K., Burge,C.B. and Bartel,D.P. (2009) Most mammalian mRNAs are conserved targets of microRNAs. *Genome Res.*, **19**, 92–105.
15. Kent,W.J., Sugnet,C.W., Furey,T.S., Roskin,K.M., Pringle,T.H., Zahler,A.M. and Haussler,D. (2002) The human genome browser at UCSC. *Genome Res.*, **12**, 996–1006.
16. Pruitt,K.D., Tatusova,T. and Maglott,D.R. (2007) NCBI reference sequences (RefSeq): a curated non-redundant sequence database of genomes, transcripts and proteins. *Nucleic Acids Res.*, **35**, D61–D65.
17. Lewis,B.P., Burge,C.B. and Bartel,D.P. (2005) Conserved seed pairing, often flanked by adenosines, indicates that thousands of human genes are microRNA targets. *Cell*, **120**, 15–20.
18. Schwartz,S., Elnitski,L., Li,M., Weirauch,M., Riemer,C., Smit,A., Green,E.D., Hardison,R.C. and Miller,W. (2003) MultiPipMaker and supporting tools: Alignments and analysis of multiple genomic DNA sequences. *Nucleic Acids Res.*, **31**, 3518–3524.
19. Livak,K.J. and Schmittgen,T.D. (2001) Analysis of relative gene expression data using real-time quantitative PCR and the 2(-Delta Delta C(T)) Method. *Methods*, **25**, 402–408.
20. Muro,A.F., Chauhan,A.K., Gajovic,S., Iaconcig,A., Porro,F., Stanta,G. and Baralle,F.E. (2003) Regulated splicing of the fibronectin EDA exon is essential for proper skin wound healing and normal lifespan. *J. Cell. Biol.*, **162**, 149–160.
21. Muro,A.F., Marro,M.L., Gajovic,S., Porro,F., Luzzatto,L. and Baralle,F.E. (2000) Mild spherocytic hereditary elliptocytosis and altered levels of alpha- and gamma-adducins in beta-adducin-deficient mice. *Blood*, **95**, 3978–3985.
22. Siepel,A., Bejerano,G., Pedersen,J.S., Hinrichs,A.S., Hou,M., Rosenbloom,K., Clawson,H., Spieth,J., Hillier,L.W., Richards,S. *et al.* (2005) Evolutionarily conserved elements in vertebrate, insect, worm, and yeast genomes. *Genome Res.*, **15**, 1034–1050.
23. John,B., Enright,A.J., Aravin,A., Tuschl,T., Sander,C. and Marks,D.S. (2004) Human microRNA targets. *PLoS Biol.*, **2**, e363.
24. Xie,X., Lu,J., Kulbokas,E.J., Golub,T.R., Mootha,V., Lindblad-Toh,K., Lander,E.S. and Kellis,M. (2005) Systematic discovery of regulatory motifs in human promoters and 3′ UTRs by comparison of several mammals. *Nature*, **434**, 338–345.
25. Giraldez,A.J., Mishima,Y., Rihel,J., Grocock,R.J., Van Dongen,S., Inoue,K., Enright,A.J. and Schier,A.F. (2006) Zebrafish MiR-430 promotes deadenylation and clearance of maternal mRNAs. *Science*, **312**, 75–79.
26. Wakiyama,M., Takimoto,K., Ohara,O. and Yokoyama,S. (2007) Let-7 microRNA-mediated mRNA deadenylation and translational repression in a mammalian cell-free system. *Genes Dev.*, **21**, 1857–1862.
27. Wu,L., Fan,J. and Belasco,J.G. (2006) MicroRNAs direct rapid deadenylation of mRNA. *Proc. Natl Acad. Sci. USA*, **103**, 4034–4039.
28. Barreau,C., Paillard,L. and Osborne,H.B. (2005) AU-rich elements and associated factors: are there unifying principles? *Nucleic Acids Res.*, **33**, 7138–7150.
29. Bhattacharyya,S.N., Habermacher,R., Martine,U., Closs,E.I. and Filipowicz,W. (2006) Relief of microRNA-mediated translational repression in human cells subjected to stress. *Cell*, **125**, 1111–1124.
30. Kedde,M., Strasser,M.J., Boldajipour,B., Oude Vrielink,J.A., Slanchev,K., le Sage,C., Nagel,R., Voorhoeve,P.M., van Duijse,J., Orom,U.A. *et al.* (2007) RNA-binding protein Dnd1 inhibits microRNA access to target mRNA. *Cell*, **131**, 1273–1286.
31. Igea,A. and Mendez,R. (2010) Meiosis requires a translational positive loop where CPEB1 ensues its replacement by CPEB4. *EMBO J.*, **29**, 2182–2193.
32. Tanzer,A. and Stadler,P.F. (2004) Molecular evolution of a microRNA cluster. *J. Mol. Biol.*, **339**, 327–335.
33. Ventura,A., Young,A.G., Winslow,M.M., Lintault,L., Meissner,A., Erkeland,S.J., Newman,J., Bronson,R.T., Crowley,D., Stone,J.R. *et al.* (2008) Targeted deletion reveals essential and overlapping functions of the miR-17–92 family of miRNA clusters. *Cell*, **132**, 875–886.
34. Huse,J.T., Brennan,C., Hambardzumyan,D., Wee,B., Pena,J., Rouhanifard,S.H., Sohn-Lee,C., le Sage,C., Agami,R., Tuschl,T. *et al.* (2009) The PTEN-regulating microRNA miR-26a is amplified in high-grade glioma and facilitates gliomagenesis in vivo. *Genes Dev.*, **23**, 1327–1337.
35. Sander,S., Bullinger,L., Klapproth,K., Fiedler,K., Kestler,H.A., Barth,T.F., Moller,P., Stilgenbauer,S., Pollack,J.R. and Wirth,T. (2008) MYC stimulates EZH2 expression by repression of its negative regulator miR-26a. *Blood*, **112**, 4202–4212.
36. Bartel,D.P. (2009) MicroRNAs: target recognition and regulatory functions. *Cell*, **136**, 215–233.
37. Costessi,L., Devescovi,G., Baralle,F.E. and Muro,A.F. (2006) Brain-specific promoter and polyadenylation sites of the beta-adducin pre-mRNA generate an unusually long 3′-UTR. *Nucleic Acids Res.*, **34**, 243–253.
38. Ji,Z., Lee,J.Y., Pan,Z., Jiang,B. and Tian,B. (2009) Progressive lengthening of 3′ untranslated regions of mRNAs by alternative polyadenylation during mouse embryonic development. *Proc. Natl Acad. Sci. USA*, **106**, 7028–7033.
39. Sandberg,R., Neilson,J.R., Sarma,A., Sharp,P.A. and Burge,C.B. (2008) Proliferating cells express mRNAs with shortened 3′ untranslated regions and fewer microRNA target sites. *Science*, **320**, 1643–1647.
40. Mayr,C. and Bartel,D.P. (2009) Widespread shortening of 3′UTRs by alternative cleavage and polyadenylation activates oncogenes in cancer cells. *Cell*, **138**, 673–684.
41. Lee,J.Y., Yeh,I., Park,J.Y. and Tian,B. (2007) PolyA_DB 2: mRNA polyadenylation sites in vertebrate genes. *Nucleic Acids Res.*, **35**, D165–D168.
42. Thorrez,L., Tranchevent,L.C., Chang,H.J., Moreau,Y. and Schuit,F. (2010) Detection of novel 3′ untranslated region extensions with 3′ expression microarrays. *BMC Genomics*, **11**, 205.